JOURNAL OF SOLID STATE CHEMISTRY 46, 373–381 (1983)

Supercell Ordering in a Hollandite-type Phase: Potassium Magnesium Antimony Oxide

A. PRING, DAVID J. SMITH*, AND D. A. JEFFERSON

*Department of Physical Chemistry, University of Cambridge, Lensfield Road, Cambridge CB2 1EP, and *High Resolution Electron Microscope, University of Cambridge, Free School Lane, Cambridge, CB2 3RQ, United Kingdom*

Received October 4, 1982

The hollandite-type phase $K_{1.33}Mg_{3.11}Sb_{4.89}O_{16}$ has been studied by X-ray and electron diffraction as well as high resolution electron microscopy at 500 kV. This material was found to adopt the tetragonal hollandite structure, space group $I4/m$, with $a = 10.315$ (4) Å; $c = 3.080$ (4) Å. The formation of a $3c$ body-centered supercell was observed and this was shown to be due to ordering of potassium cations within the tunnel sites. Computer image simulations established that ordering of the tunnel cations alone rather than the octahedrally coordinated framework cations was responsible for superlattice formation. In some crystals the supercell ordering appeared to occur in domains.

Introduction

A chemically diverse variety of hollandite-type phases are known. The "hollandite" polymorph of sanidine feldspar, $KAlSi_3O_8$, has been proposed as a major phase of the Earth's mantle, while the mineral hollandite, $BaMn_8O_{16}$, and other manganese oxide hollandite-type minerals are important constituents of manganese deposits. Synthetic hollandite-type phases have been examined as possible solid state electrolytes (*1*) and superionic conductors (*2*). The use of a hollandite-type phase, $BaAl_2Ti_6O_{16}$, as a host for radioactive cesium in the nuclear waste disposal material called "SYNROC" has also been proposed (*3*).

The basis of the hollandite structure (from the mineral hollandite, $BaMn_8O_{16}$ (*4*)) is the square tunnel enclosed by columns of two edge-sharing octahedra which, in turn, share corners to form two-by-two tunnels running parallel to the short, high-symmetry, axis of the structure. This is illustrated schematically in Fig. 1. These tunnels accommodate large cations, potassium in this case, which are introduced to balance excess charge resulting from substitutions in the octahedral sites of the MO_2 framework. Noninteger numbers of tunnel cations are common in hollandite-type phases (there being two tunnel sites in the body-centered unit cell) and partial occupancy of these sites may lead to superlattice formation.

A variety of commensurate and incommensurate ordering schemes have been reported: a doubling of c was observed in the

0022-4596/83/030373-09$03.00/0

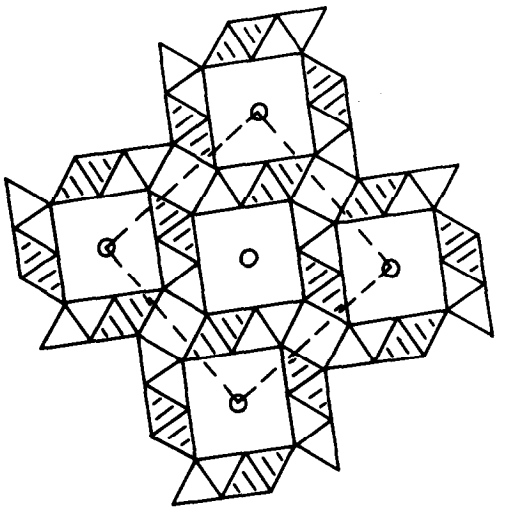

FIG. 1. Hollandite structure projected down the fourfold axis onto the (001) plane: edge-sharing pairs of MO_6 octahedra share corners to produce square tunnels occupied by potassium ions. The body-centered unit cell is outlined.

mineral hollandite (*5*); a 3*c* primitive supercell in $Ba_{1.3}Cr_{2.6}Ru_{5.4}O_{16}$ (*6*); and a number of incommensurate superlattices in the $Ba_xMg_xTi_{8-x}O_{16}$ and $Ba_xGa_{2x}Ti_{8-2x}O_{16}$ series based on the intergrowth of 2*c*, 3*c* primitive, and 5*c* body-entered supercells (*7*). The formation of a commensurate superlattice in $K_{1.33}Mg_{3.11}Sb_{4.89}O_{16}$ has also been noted (*8*). Recently a 3*c* body-centered supercell for $K_{1.8}(Li_{2.45}Sb_{5.55})O_{16}$ was reported although, due to the diffuseness of the superlattice reflections, the structure of the ordered supercell could not be refined.

We report here an investigation into superlattice formation in the potassium magnesium antimony oxide phase, $K_{1.33}Mg_{3.11}Sb_{4.89}O_{16}$, using both electron diffraction and high resolution electron microscopy. Possible ordering schemes were postulated and a comparison of computed images with experimental micrographs could then be used to establish the nature of the superlattice. A preliminary report of some of this work has been given elsewhere (*10*).

Experimental

Stoichiometric amounts of K_2O, MgO, and Sb_2O_5 were ground together and sealed in a Pt tube. The mixture was then heated to 1250° for 48 hr, followed by slow cooling, 10°C/hr, to room temperature. No crystals large enough (ca. 0.1 mm) for use in a conventional structure refinement by single crystal X-ray diffraction methods were found in the product although examination by powder X-ray diffraction was possible.

Initial electron diffraction and high resolution imaging studies were performed using a JEOL 200CX electron microscope fitted with a side-entry double-tilt goniometer and facilities for spectral analysis using an energy-dispersive X-ray spectrometer (E.D.A.X.). High resolution electron micrographs were also obtained with the Cambridge University high resolution electron microscrope (HREM) (*11*). The spherical, C_s, and chromatic, C_c, aberration coefficients of this instrument were $C_s \sim 2.7$ mm, $C_c \sim 2.9$ mm, giving a directly interpretable image resolution of ~2.0 Å for operation at 500 kV.

Specimens suitable for electron microscopy were prepared in the normal manner by grinding in an agate mortar and mounting on holey carbon films. Image astigmatism and beam alignment were corrected by direct observation of support film granularity at magnifications typically of 600,000 to 750,000 times.

Image simulations for the HREM operating conditions were based on the multislice method (*12*), and used an IBM 370 computer with programs written by one of us (D.A.J.). The maximum number of beams included in the calculation of diffracted intensities was 109, although the relatively weak beams lying beyond the first zero of the contrast transfer function (~2.0 Å) at optimum defocus were normally omitted from the final image since they were found to have little influence on the image contrast.

Results

Observations of Superlattice

The oxide phase was found by X-ray diffraction to have the tetragonal hollandite structure, space group $I4/m$. A least squares refinement of the 20 strongest powder lines gave cell parameters $a = 10.315$ (4) Å and $c = 3.080$ (4) Å, with corresponding volume $V = 327.8$ Å^3. This last figure is significant since it has been predicted (*13*) that hollandites with unit cell volumes greater than about 300 Å^3 will have a monoclinic distortion. However, no evidence was found here for any such distortion in this potassium magnesium antimony oxide hollandite phase.

Electron diffraction patterns from several zones of the hollandite phase, namely [001], [100], and [103], are shown in Fig. 2a–c. The [001] zone axis displays a sharp, square array of diffraction spots, characteristic of the fourfold axis of the hollandite structure, whereas the [100] and [103] zones show strong superlattice reflections. The superlattice multiplicity (m) was found to be $3 \times d_{002}$ in the [100] zone and $3 \times d_{30\bar{1}}$ in the [103] zone, thus signifying an $a \times a \times 3c$ body-centered supercell. The relative sharpness of the superlattice reflections in [100] and [010] directions implies that the

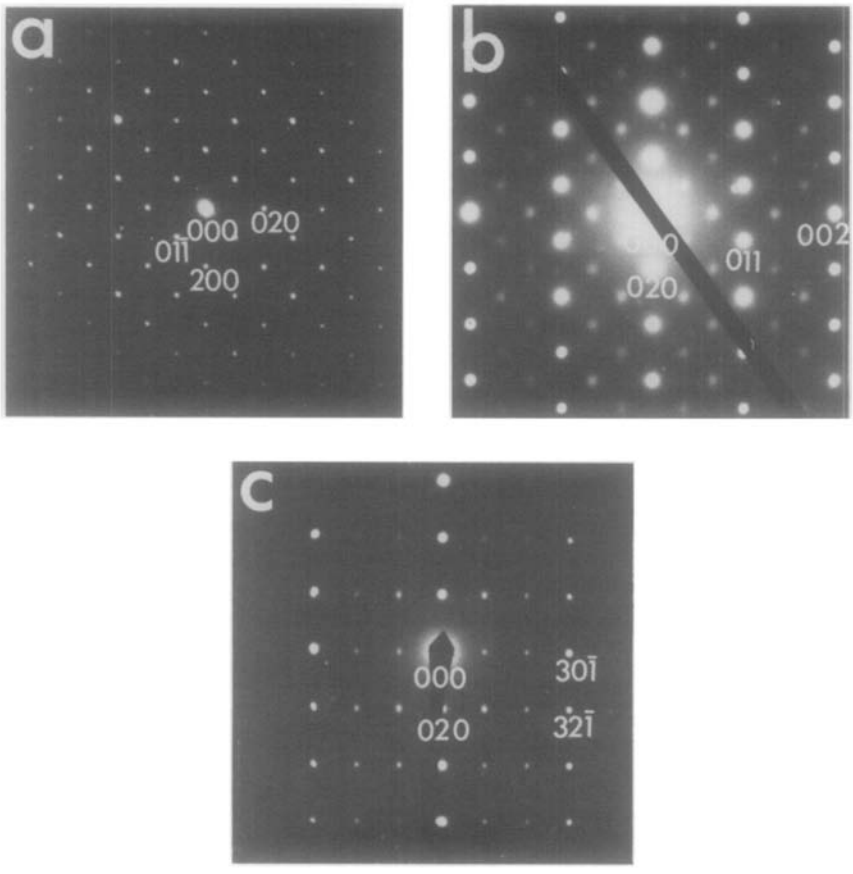

FIG. 2. Electron diffraction patterns from $K_{1.33}Mg_{3.11}Sb_{4.89}O_{16}$ crystals: (a) [001] zone; (b) [100]; (c) [103]. Note the superlattice reflections tripling (002) in the [100] zone, and (30$\bar{1}$) in the [103] zone.

ordering sequence within adjacent tunnels is quite well correlated.

High resolution electron micrographs were recorded at 500 kV in three zones, namely [001], [100], and [213], for comparison with image simulations (see later) to establish whether the superlattice was a result of framework ordering or due solely to ordering of potassium ions in the tunnel sites. Figure 3 shows an image taken in the [001] zone which is similar to those recorded at 100 kV by Bursill and Wilson (*14*), although at somewhat better resolution. The detail at the thin crystal edge can be readily interpreted in terms of the hollandite structure using the projected-charge density approximation (*15*); separation of the centers of the pairs of edge-sharing octahedra can be clearly observed. Figure 4 shows a micrograph recorded down the [100] direction, which is perpendicular to the length of the tunnels. The $3 \times c$ periodicity is not particularly prominent but is visible when viewed obliquely along the [011] direction (arrowed). Crystals in this orientation were found to be composed of ordered domains of up to several hundred unit cells in size—domain boundaries can also be located by viewing along [011]. An image recorded in the [213] zone is shown in Fig. 5. The tripling of the cell is clearly visible in this projection as is the extent of the ordered domains.

Ordering Schemes

At the stoichiometry of an oxide phase with composition given by $K_{1.33}Mg_{3.11}Sb_{4.89}O_{16}$, only two thirds of the two tunnel sites in the simple hollandite cell are occupied. Four arrangements of the four potassium ions over the six tunnel sites in a $3c$ supercell are then possible, which we will call OR I–IV, and these are illustrated schematically in Fig. 6. In the first

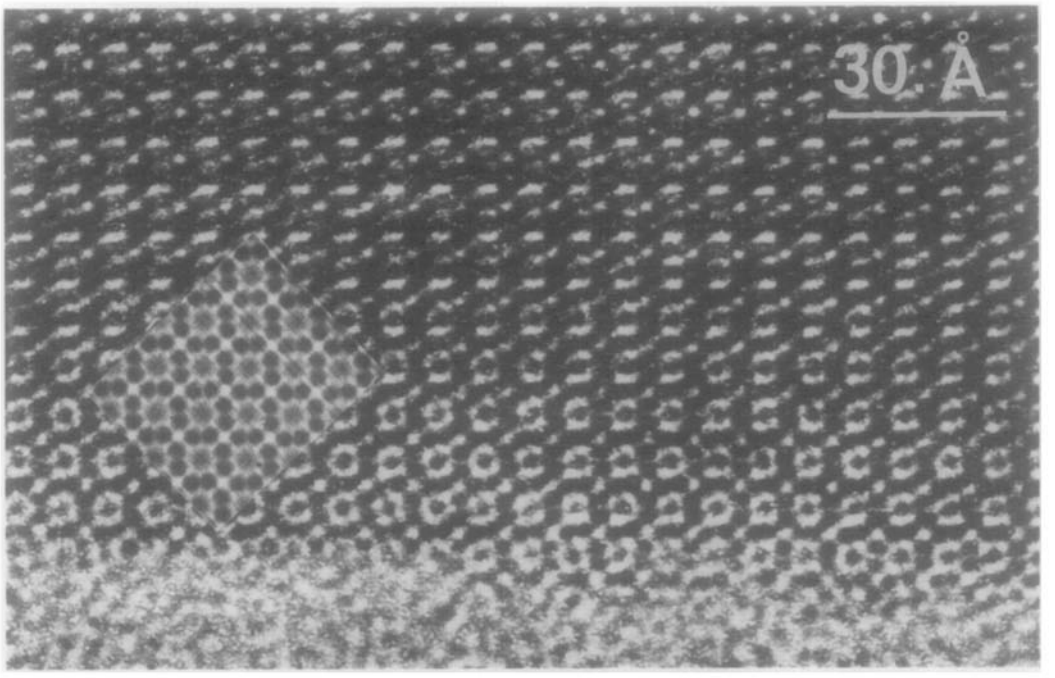

FIG. 3. High resolution lattice image of the hollandite taken down the [001] zone. Inserted is the matching image simulation for a crystal of thickness 25 Å and objective lens defocus of −550 Å.

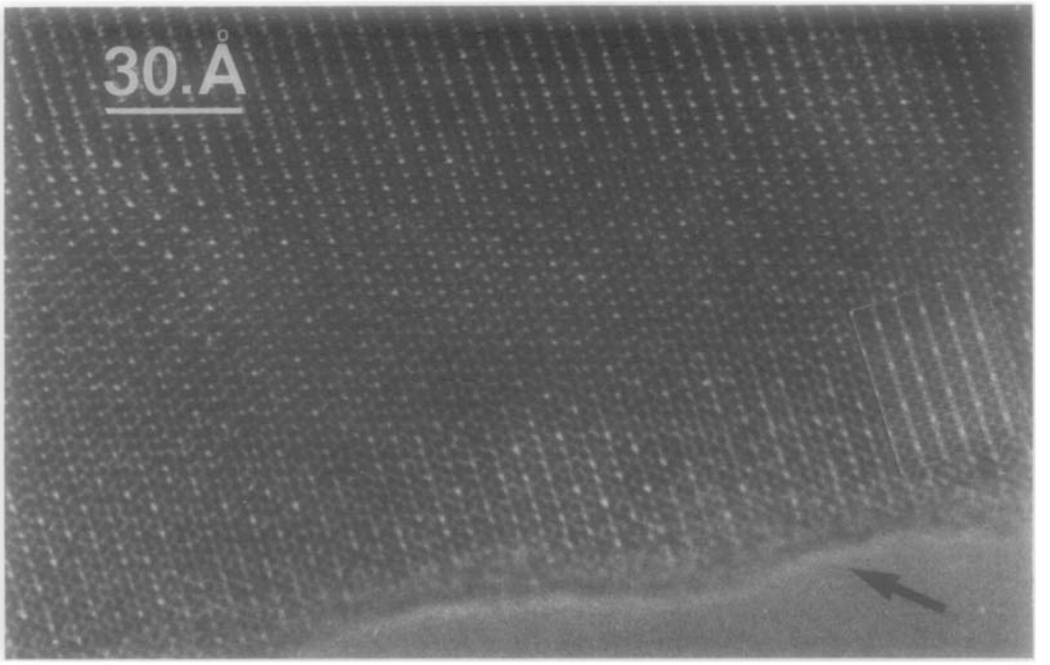

FIG. 4. Lattice image of $K_{1.33}Mg_{3.11}Sb_{4.89}O_{16}$ down [100]. This lattice image was matched by computer simulation using the tunnel-cation-ordered framework-disordered model for a thickness of 25 Å at −580 Å defocus (see inset). The 3*c* supercell repeat can be readily observed when the image is viewed along the [011] direction (arrowed). The boundaries between the ordered domains can also be observed along this direction.

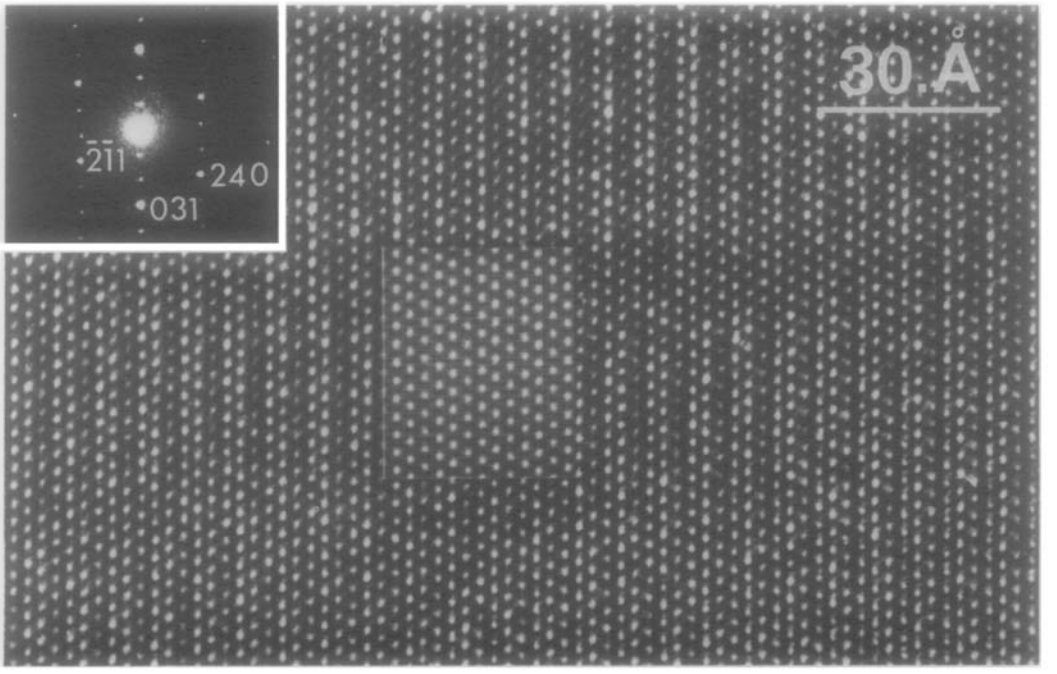

FIG. 5. Image recorded down [213] of the hollandite phase. The three times supercell repeat is readily seen, and every third row of white blobs is brighter. The inserted image simulation was calculated for a crystal 50 Å thick at a defocus of −400 Å.

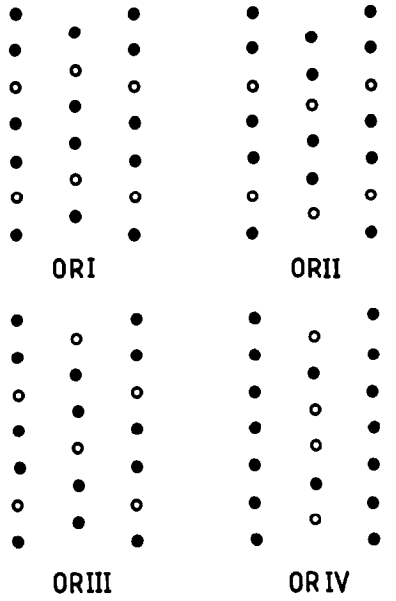

FIG. 6. Schematic diagram of the hollandite structure projected down [100]—tunnel cation sites only are shown: filled circles denote occupied sites; open circles denote vacancies. ORI to ORIV are the four possible ordering schemes for tunnel cations to give $3c$ supercells. Ordering Schemes ORI and II are equivalent, differing only in choice of origin. These schemes correspond to a $3c$ primitive supercell as does ORIV. In ordering scheme III the vacant sites have a body-centered distribution corresponding to a $3 \times c$ body-centered supercell.

three of these ordering schemes, each tunnel contains sequences with a pair of occupied sites separated by a vacancy. In ORI and ORII, the phase shift between tunnels is $\frac{1}{2}c$, resulting in a primitive supercell, whereas ORIII has a phase shift of $1\frac{1}{2}c$ between ordering sequences in the tunnels leading to a body-centered $3c$ supercell. Finally, the scheme ORIV contains alternate rows of tunnels which are either completely filled or which contain pairs of vacancies separated by an occupied site. Of these various ordering schemes, only ORIII is body-centered and could produce the observed superlattice. The other three ordering schemes would produce $m = 6$ superlattices, as observed for hollandite phase $Ba_{1.3}Cr_{2.6}Ru_{5.4}O_{16}$ (*6*). Supercells of the type ORI and ORII have been found as component supercells responsible for the incommensurate superlattices observed in $Ba_xMg_xTi_{8-x}O_{16}$ and $Ba_xGa_{2-x}Ti_{8-2x}O_{16}$ (*7*).

The cation ordering scheme ORIII is not the only possible ordered structure which could result in the observed superlattice since the framework of the hollandite could also be ordered into a c body-centered supercell. This can be understood by first con-

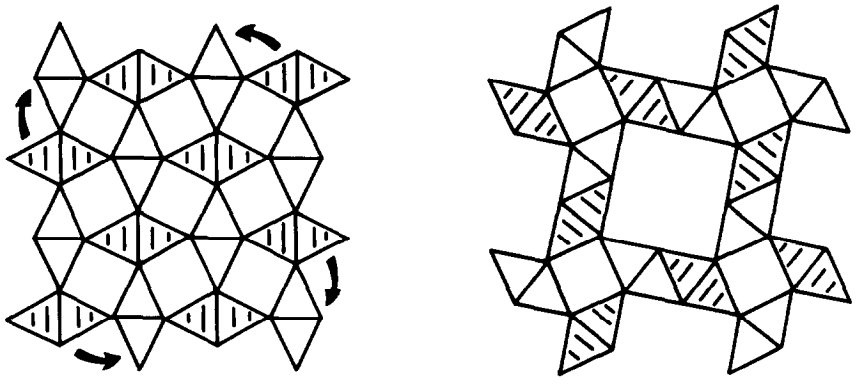

FIG. 7. Structural diagrams of rutile (a) and hollandite (b) illustrating the relationship between the two structures. Rotations of columns of octahedra in rutile by $\pi/4$ radians in alternatively clockwise and anticlockwise direction, shown by the arrows, generate the hollandite structure.

sidering the structural relationship between the rutile and hollandite structures (e.g., (*16*)). The hollandite structure can be derived from rutile by $\pi/4$ rotations of successive columns of TiO_2 octahedra in alternate directions: the corner-sharing octahedra of the rutile structure then share edges in such a way that the stoichiometry remains MO_2 (see Fig. 7). Whilst there is no simple structural analog of rutile in either the antimony oxide or magnesium antimony oxide systems, the magnesium diantimony oxide, $MgSb_2O_6$, has the trirutile structure consisting of three superimposed rutile layers. Trirutile structures, although primitive, space group $P4_2/mnm$, have a body-centered distribution of metal cations {Mg(0,0,0; $\frac{1}{2},\frac{1}{2},\frac{1}{2}$); Sb(0,0, $\pm z$; $\frac{1}{2},\frac{1}{2},\frac{1}{2} \pm z$) and thus a body-centered $3c$ hollandite supercell could be generated directly by rotary shear of the trirutile structure in the same manner as the simple hollandite cell can be derived from rutile. The resulting $3c$ supercell contains an ordered body-centered distribution of cations in the octahedral sites; those derived from the magnesium sites of trirutile would contain exclusively magnesium while those derived from the antimony sites would, by necessity, have a magnesium occupancy of $\frac{1}{8}$ (the magnesium being introduced to maintain charge balance when the potassium ions occupy the cubic tunnel sites).

Three possible structural models can then be proposed to explain the body-centered $3c$ ordered superlattice observed in the potassium magnesium antimony oxide: the first is based on an ordering of the tunnel cations alone into a $3c$ body-centered supercell with a disordered framework; in the second, both the framework and tunnel cations are ordered into a supercell; finally, the framework cations are ordered and the tunnel cations disordered.

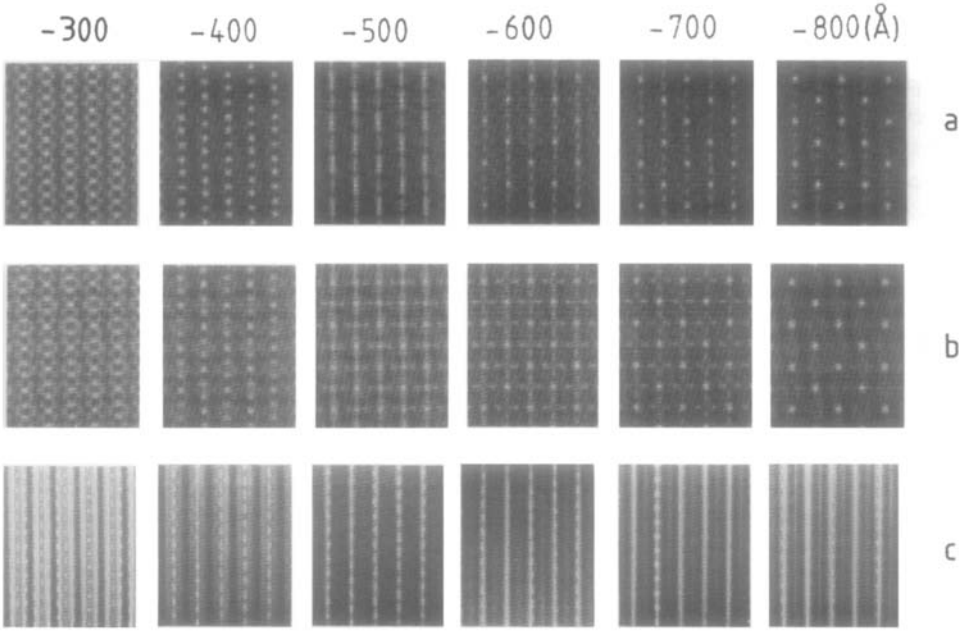

FIG. 8. [100] zone through-focal series of image simulations for the hollandite using the three proposed ordering models at a thickness of 25 Å. (a) tunnel cations ordered, framework disordered, (b) tunnel and framework cations ordered, (c) tunnel cations disordered and framework ordered.

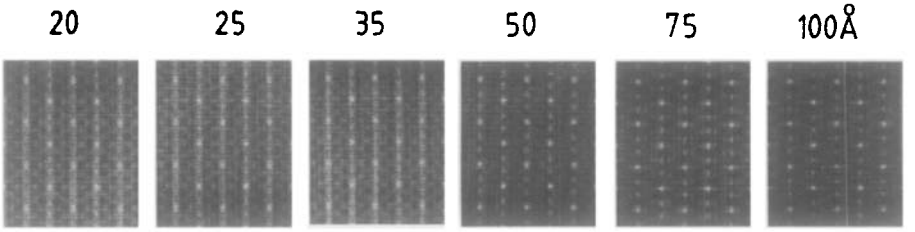

FIG. 9. Through-thickness series of image simulations calculated using the matching model (tunnel cations ordered, framework disordered) at a defocus of −600 Å.

Image Simulations

Atomic coordinates for the three structural models were derived from the coordinates of the simple cell, and used in image calculations. Fig. 8a–c shows a through focal series of images simulated for each of the models projected down [100] for a crystal thickness of 25 Å. A close image match with Fig. 4 was obtained for the structural model with tunnel ordering only (ORIII) at a defocus of −580 Å (see inset to Fig. 4). Image detail along the [100] projection changes rapidly with increases in thickness so images at several other thicknesses for model ORIII were also calculated (Fig. 9). Good agreement between experimental and simulated images was obtained up to a thickness of 100 Å, whereas no satisfactory match could be obtained using the other models. Further confirmation of the proposed ordering scheme was obtained by simulation of images for the [213] zone: as shown by the inset to Fig. 5, good agreement with the experimental micrograph was again obtained.

Discussion

The major objective of the present study was to account for the observed superlattice in terms of cation ordering in the hollandite structure. Indeed, comparisons between direct lattice imaging and computer image simulations have established, unambiguously, that the 3*c* body-centered supercell is due to the ordering of potassium ions in the tunnel sites. However, the high degree of lateral correlation observed in this plane is unusual since superlattice reflections for other potassium-bearing hollandites, particularly those with a titanate-based framework, tend to be diffuse streaks rather than sharp spots (*8*). It appears that the interaction between the positively charged potassium ions is sufficiently strong to overcome the shielding effects of the framework in the magnesium antimony hollandite but not in the magnesium titanium hollandites.

The potassium ions in the body-centered 3*c* supercell are arranged in pairs along the tunnels, with each pair separated from the next by a vacancy. Electrostatic interactions between potassium ions would then be expected to result in displacement of the ions from their ideal sites towards the vacancies. It is interesting that recent crystal structure refinements of hollandite-type compounds have revealed significant displacements of tunnel cations from a 2(*b*) site (0,0,½) to a 4(*e*) site (0,0, ± *z*), where *z* is ~0.30 (*9, 13, 17, 18*). Such displacements increase the K^+–K^+ separation to ~4.28 Å along the tunnel axis, thereby minimizing the electrostatic repulsions between cations.

Finally, it is somewhat surprising that the framework of this hollandite phase does not appear to order into layers thereby producing a direct hollandite analog of the trirutile phase, $MgSb_2O_6$. Bursill and Grzinic (*7*)

have previously noted, however, that rutile and thus hollandite have a natural tendency towards 3*c* supercells because of the strong 3*c* transverse acoustic mode observed in rutile phases (*19*).

Acknowledgments

The support of A.E.R.E., Harwell, the University of Cambridge, and S.E.R.C. is gratefully acknowledged. We are grateful to Professor J. M. Thomas for advice and encouragement and to Dr. L. A. Bursill for assistance in the initial stages of this study.

References

1. P. HAGENMULLER AND W. VAN GOOL. "Solid Electrolytes," p. 381. Academic Press, New York/London.
2. H. U. BEYELER, *Phys. Rev. Lett.* **37,** 1557 (1976).
3. A. E. RINGWOOD, "Safe Disposal of High Level Nuclear Reactor Wastes: A New Strategy," Australia National Univ. Press, Canberra (1978).
4. A. BYSTROM AND A. M. BYSTROM, *Acta Crystallogr.* **3,** 146 (1950).
5. B. MUKHERJEE, *Acta Crystallogr.* **13,** 164 (1960).
6. M-C. CADEE AND A. PRODAN, *Mat. Res. Bull.* **14,** 613 (1979).
7. L. A. BURSILL AND G. GRZINIC, *Acta Crystallogr. Sect. B* **36,** 2902 (1980).
8. H. U. BEYELER AND C. SCHULER, *Solid State Ionics* **1,** 77 (1980).
9. H. WATELET, J-P, BESSE, G. BAUD, AND R. CHEVALIER, *Mat. Res. Bull.* **19,** 863 (1982).
10. A. PRING, D. A. JEFFERSON, AND D. J. SMITH, *in* "Proceedings of the Second European Solid State Conference," in press.
11. D. J. SMITH, R. A. CAMPS, V. E. COSSLETT, L. A. FREEMAN, W. O. SAXTON, W. C. NIXON, H. AHMED, C. J. D. CATTO, J. R. A. CLEAVER, K. C. A. SMITH, AND A. E. TIMBS, "Ultramicroscopy," **9,** 203 (1982).
12. P. GOODMAN AND A. F. MOODIE, *Acta Crystallogr. Sect. A* **30,** 280 (1979).
13. W. SINCLAIR, G. M. MCLAUGHLIN, AND A. E. RINGWOOD, *Acta Crystallogr. Sect. B* **36,** 2913 (1980).
14. L. A. BURSILL AND A. R. WILSON, *Acta Crystallogr. Sect. A* **33,** 672 (1977).
15. D. F. LYNCH, A. F. MOODIE, AND M. A. O'KEEFE, *Acta Crystallogr. Sect. A* **31,** 300 (1975).
16. L. A. BURSILL, *Acta Crystallogr. Sect. B* **35,** 530 (1979).
17. W. SINCLAIR AND G. M. MCLAUGHLIN, *Acta Crystallogr. Sect. B* **38,** 245 (1982).
18. J. E. POST, R. B. VON DREELE, AND P. R. BUSECK, *Acta Crystallogr. Sect. B* **38,** 1056 (1982).
19. J. G. TRAYLOR, H. G. SMITH, R. M. NICKLOW, AND M. K. WILKINSON, *Phys. Rev. B* **3,** 3457 (1971).